Journal of Hydrology 554 (2017) 635–645

Contents lists available at ScienceDirect

Journal of Hydrology

journal homepage: www.elsevier.com/locate/jhydrol

Research papers

Hydrological responses to climatic changes in the Yellow River basin, China: Climatic elasticity and streamflow prediction

Qiang Zhang [a,b,c,*], Jianyu Liu [d,*], Vijay P. Singh [e], Peijun Shi [a,b,c], Peng Sun [f]

[a] Key Laboratory of Environmental Change and Natural Disaster, Ministry of Education, Beijing Normal University, Beijing 100875, China
[b] State Key Laboratory of Earth Surface Processes and Resource Ecology, Beijing Normal University, Beijing 100875, China
[c] Faculty of Geographical Science, Academy of Disaster Reduction and Emergency Management, Beijing Normal University, Beijing 100875, China
[d] Department of Water Resources and Environment, Sun Yat-sen University, Guangzhou 510275, China
[e] Department of Biological and Agricultural Engineering and Zachry Department of Civil Engineering, Texas A&M University, College Station, TX, USA
[f] College of Terrestrial Resources and Tourism, Anhui Normal University, 241000 Anhui, China

ARTICLE INFO

Article history:
Received 15 June 2017
Received in revised form 20 August 2017
Accepted 22 September 2017
Available online 28 September 2017

Keywords:
Budyko framework
GCMs
Climatic scenarios
Streamflow prediction
Uncertainty

ABSTRACT

Prediction of streamflow of the Yellow River basin was done using downscaled precipitation and temperature based on outputs of 12 GCMs under RCP2.6 and RCP8.5 scenarios. Streamflow changes of 37 tributaries of the Yellow River basin during 2070–2099 were predicted related to different GCMs and climatic scenarios using Budyko framework. The results indicated that: (1) When compared to precipitation and temperature during 1960–1979, increasing precipitation and temperature are dominant during 2070–2099. Particularly, under RCP8.5, increase of 10% and 30% can be detected for precipitation and temperature respectively; (2) Precipitation changes have larger fractional contribution to streamflow changes than temperature changes, being the major driver for spatial and temporal patterns of water resources across the Yellow River basin; (3) 2070–2099 period will witness increased streamflow depth and decreased streamflow can be found mainly in the semi-humid regions and headwater regions of the Yellow River basin, which can be attributed to more significant increase of temperature than precipitation in these regions; (4) Distinctly different picture of streamflow changes can be observed with consideration of different outputs of GCMs which can be attributed to different outputs of GCMs under different scenarios. Even so, under RCP2.6 and RCP8.5 scenarios, 36.8% and 71.1% of the tributaries of the Yellow River basin are dominated by increasing streamflow. The results of this study are of theoretical and practical merits in terms of management of water resources and also irrigated agriculture under influences of changing climate.

1. Introduction

In the backdrop of global warming, intensifying hydrological cycle at regional and global scales (IPCC, 2007), water security that has the potential to result in regional-scale consequences for economies and vulnerable ecosystems as well (Bates et al., 2008). Besides, enhancing human impacts on streamflow changes due to intensifying human activities (Zhang et al., 2015a), and particularly importance of availability and variability of water resources underlined by sustainable development of human society, have aroused international interests in investigation of effects of climate changes and human activities on hydrological processes (Arnell and Gosling, 2013; Li et al., 2013; Zhou et al., 2014; Li et al., 2016; Kumar et al., 2016). Generally, precipitation was accepted as a major driver modifying streamflow processes (Novotny and Stefan, 2007; Zhang et al., 2016) and which was well corroborated by Ryberg et al. (2013) and Frans et al. (2013) based on their study on streamflow changes over the U.S. Midwest.

However, human impacts on streamflow changes, such as agricultural irrigation (Li et al., 2017a,b), impoundment effects of water reservoirs (Yang et al., 2008b), have attracted increasing human concerns in recent years (Ahn and Merwade, 2014; Zhang et al., 2015a). Analyzing precipitation vs. streamflow relations across China, Zhang et al. (2015a) indicated that influences of human activities and precipitation changes on streamflow were different for different river basins. Modelling and prediction of streamflow in a changing environment is hence a critical issue for basin-scale water resources management.

* Corresponding authors at: Academy of Disaster Reduction and Emergency Management, Ministry of Education, Beijing Normal University, Beijing 100875, China (Q. Zhang); Sun Yat-sen University, Guangzhou 510275, China (J.Y. Liu).
E-mail addresses: zhangq68@bnu.edu.cn (Q. Zhang), liujy25@mail2.sysu.edu.cn (J. Liu).

https://doi.org/10.1016/j.jhydrol.2017.09.040
0022-1694/

Climate elasticity methods were widely used in evaluation of impacts of climate variability and human activities on streamflow change (Yang et al., 2008a,b; Yang et al., 2014; Huang et al., 2016; Kumar et al., 2016; Wang et al., 2016; Liu et al., 2017). Assessing the rainfall elasticity of streamflow in 219 catchments across Australia, Chiew (2006) found that the results from climate elasticity are in good line with those by hydrological modelling approach. Teng et al. (2012) further indicated that hydrological modelling techniques are not necessarily more reliable than those estimated from the climatic elasticity methods in the projected long-term streamflow changes. Sankarasubramanian et al. (2001) summarized five categories of approaches for calculation of the climatic elasticity, and they illustrated that the analytical derivation has a specific theoretical basis, i.e., analytical derivation based on the Budyko framework. This constitutes the major motivation of this current study, i.e. to predict streamflow changes using climatic elasticity method based on Budyko framework in the Yellow River basin, being characterized by intensifying human activities and by serious water shortage.

The Yellow River (95 °53′E-119 °5′E; 32 °10′N-41 °50′N) (Fig. 1) is the second largest river in China and the fifth largest river in the world. The length of the Yellow River is 5464 km with drainage area of 752440 km^2, running through the arid and semi-arid region (Zhang et al., 2009b). The Yellow River basin is the major source for water supply in the North-western China and Northern China, however it is also the area of shortage of water resource (Wang et al., 2001; Zhang et al., 2009b). Since 1986, due to climatic change and intensifying human activities, particularly increasing human withdrawal of water because of increasing agriculture irrigation, the streamflow of the lower Yellow River has significantly decreased (Xu, 2002). Annual precipitation over the Yellow River basin has been in decreasing tendency since the 1970s, which together with increasing abstraction from the Yellow River leads frequent desiccation (dry up) (Xu, 2001). However, it should be noted here that the Yellow River basin, with drainage area of 75.3×10^4 km^2, supplies water to 12% of the population of China, but the significant decreases in its streamflow, particularly since the 1990s, is now the focus of considerable concern (Zhang et al., 2009b; Li et al., 2017a,b).

Actually, there are numerous researches addressing streamflow changes of the Yellow River and related causes behind. Particularly, more importance has been attached to differentiation of climatic and human impacts on streamflow changes across the Yellow River basin. Although there are many researches addressing individual contributions of climatic changes and human activities to streamflow changes (Wang et al., 2012a,b; Tang et al., 2013), a majority of researches have focused on either the influence of human activities, such as building of water reservoirs (e.g. Yang et al., 2008a, b) and soil conservation measures (Liang et al., 2013), or of climatic changes, e.g. precipitation and temperature, on streamflow variation (Tang et al., 2013). Liu and Cui (2011) applied climate elasticity approach to assess impacts of precipitation and potential evaporation on streamflow change during 1961–2000. Zheng et al. (2009) found that streamflow changes in the Yellow River based are more sensitive to precipitation than to potential evapotranspiration during 1960–2000. Li et al. (2017a,b) investigates the changing properties and underlying causes for the decreased streamflow by applying streamflow data for the period 1960–2014 to both the Budyko framework and the hydrological modelling techniques. However, no reports have been found addressing projection of streamflow in the Yellow River basin although some standing reports focused on projection of streamflow over China (e.g. Li et al., 2016; Zhang et al., 2015b). Even so, multiple GCMs ensemble for comprehensive knowledge of future streamflow variations at regional scale across the Yellow River basin is still of theoretical and practical merits and it is particularly true for policymakers to formulate more reasonable water management policy for water resource distribution and reservoir regulation (Naz et al., 2016) in arid and semiarid river basins over the globe.

Therefore, the objectives of this study are to: (1) evaluate spatiotemporal variations of precipitation and temperature across the Yellow River basin based on outputs of 12 GCMs under RCP2.6 and RCP8.5 scenarios; and (2) to project streamflow changes of 37 tributaries of the Yellow River basin using Budyko framework. This study can help to provide theoretical and scientific grounds for water resources management in the Yellow River basin in a changing environment, enhancing human mitigation to

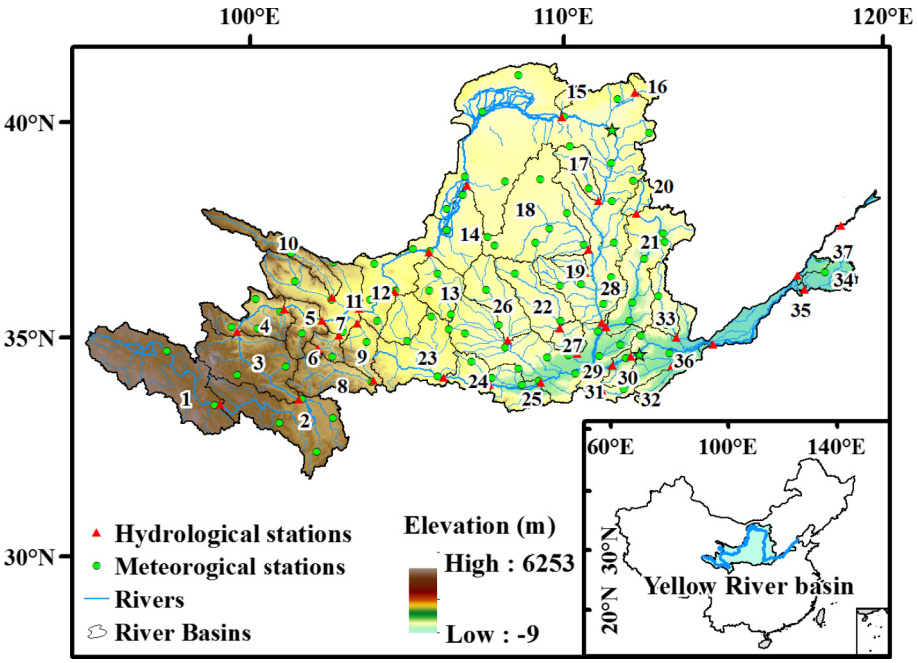

Fig. 1. Locations of the Yellow River basin and meteorological and hydrological stations.

climate impacts on water resources in arid and semiarid river basins over the globe.

2. Data

In this study, monthly streamflow during 1960–2000 were collected from 37 hydrological stations across the Yellow River basin (Fig. 1). The missing data are less than 1% of the total streamflow data and were processed using 7-year moving average method. Meteorological data during 1960–2014 were collected from 77 meteorological stations and the locations of the meteorological stations can be found in Fig. 1. The data quality was firmly controlled before its release. Prediction of streamflow was done based on precipitation data, maximum and minimum air temperature from outputs of 12 CMIP5 GCMs under RCP2.6 and RCP8.5 scenarios (Table 1) (Taylor et al., 2012). RCP2.6 scenario refers to the low emission of CO_2 with temperature increase of 2 °C and solar radiation of 3 W/m^2 in 2035–2.6 W/m^2 in 2100. RCP8.5 scenario refers to the high emission of CO_2 with increase of solar radiation to 8.5 W/m^2 in 2100 (Riahi et al., 2011; van Vuuren et al., 2011). In this study, downscaling analysis for precipitation, temperature and streamflow was done using Model Ensemble Medians (MEMs) (Reichler and Kim, 2008; Zhang et al., 2014; Li et al., 2016). Meanwhile, it has been well corroborated that GCMs can well describe changing properties of precipitation and temperature (Mehrotra et al., 2013; Chen et al., 2014; Li et al., 2016) and changes of precipitation, temperature and streamflow during 2070–2099 when compared to that during 1960–1979 were analyzed by taking the time interval of 1960–1979 as the benchmark period.

3. Methods

3.1. Budyko assumption

Budyko (1974) stated that water balance can be controlled mainly by available water volume (precipitation), potential demand of water volume (potential evapotranspiration) and can be evaluated by a semi-empirical equation as:

$$\frac{E}{P} = F\left(\frac{E_0}{P}\right) \tag{1}$$

where F is assumed as the universal function for all the river basins

Yang and Yang (2011) deduced the hydrothermal coupled balance equation based on Budyko assumption as:

$$R = P - \frac{PE_0}{(P^n + E_0^n)^{1/n}} \tag{2}$$

where n denotes the parameter reflecting features of the underlying surface, including vegetation cover and soil and so forth (Yang et al., 2008a,b; Gao et al., 2016). The n can be calibrated from historical data by minimizing the least squares errors between the simulated and observed streamflow in each individual tributary. Therefore, long-term annual average streamflow can be computed by the following complete differential equation:

$$\frac{dR}{R} = \varepsilon_P \frac{dP}{P} + \varepsilon_{E_0} \frac{dE_0}{E_0} + \varepsilon_n \frac{dn}{n} \tag{3}$$

where $\varepsilon_P = \frac{\partial f}{\partial P}\frac{P}{R}$, $\varepsilon_{E_0} = \frac{\partial f}{\partial E_0}\frac{E_0}{R}$, $\varepsilon_n = \frac{\partial f}{\partial n}\frac{n}{R}$, ε_P, ε_{E_0}, and ε_n are respectively the elasticity coefficients of precipitation (P), potential evaporation (E_0) and underlying parameter, n, to streamflow.

Impacts of climatic changes (precipitation and potential evaporation) on streamflow changes can be quantified by the following equation without considering impacts of land use and land cover changes (Yang and Yang, 2011):

$$\frac{dR}{R} = \varepsilon_P \frac{dP}{P} + \varepsilon_{E_0} \frac{dE_0}{E_0} \tag{4}$$

Eq. (4) can be used to quantify impacts of future precipitation and potential evaporation changes on streamflow variations. However, Liu and Sun (2016) indicated massive uncertainty and even error in GCMs outputs of potential evaporation. Meanwhile, to fully understand influences of temperature on streamflow changes in the backdrop of warming climate, we attempted to deduce elasticity of temperature changes to streamflow variations based on functions relations between potential evaporation and temperature. In this case, the key step is to select a model that has the good modelling performance and can also fully reflect controlling role of temperature for potential evaporation changes.

3.2. Model selection for analysis of potential evaporation

Actually, there are numerous models for estimation of potential evaporation such as FAO Penman-Montieth, Thornthwaite, Priestley-Taylor, Hargreaves, Turc and Makkink. Wherein FAO Penman-Montieth equation was widely used in evaluation of potential evaporation. However, FAO Penman-Montieth needs more variables than expected such as relative humidity, solar radiation, and wind speed and so on. For estimation of future potential evaporation, more variables from GCMs outputs will definitely introduce more uncertainty (e.g. Wang et al., 2015). The Makkink equation stems from Penman model and only needs the temperature and solar radiation data, which is a widely-used method for estimation of potential evaporation and has advantage over several other evaporation equations (Makkink, 1957). Comparisons between different equations for evaluations of potential evaporation indicated that evaluation performance of the Makkink equation is close to FAO Penman-Montieth equation, and performs better than Hargreaves and Turc equations (Xu and Singh, 2000, 2002). Moreover, Xu and Chen (2005) also indicated that Makkink equation performs better than Thornthwaite, Priestley-Taylor, and Hargreaves equations in evaluation of potential evaporation. Meanwhile, Makkink equation has been widely used in evaluations of potential evaporation in different regions over the globe with acceptable modelling performance (e.g. Winter et al., 1995; De Bruin and Lablans, 1998; Boczon et al., 2015). Thus, Makkink equation was accepted in this study for evaluation of relations between potential evaporation and temperature. The Makkink equation was:

Table 1
Details of CMIP5 model simulations used in this study.

No.	GCM	Modelling Centre	Resolution (Lon × Lat)	No.	GCM	Modelling Centre	Resolution (Lon × Lat)
1	BCC-CSM1.1 (m)	BCC	320 × 160	7	CSIRO-Mk3.6.0	CSIRO-QCCCE	192 × 90
2	BNU-ESM	GCESS	128 × 64	8	GFDL-CM3	NOAA GFDL	144 × 143
3	CanESM2	CCCma	128 × 64	9	IPSL-CM5A-MR	IPSL	144 × 128
4	CCSM4	NCAR	288 × 192	10	MIROC5	TUT NIES	256 × 128
5	CESM1 (CAM5)	NSF-DOE-NCAR(1)	288 × 128	11	MPI-ESM-MR	MPI-M	192 × 96
6	CNRM-CM5	CNRM-CERFACS	256 × 96	12	MRI-CGCM3	MRI	320 × 160

$$E_0 = 0.61\frac{\Delta}{\Delta+\gamma}\frac{R_s}{\lambda} - 0.12 \quad (5)$$

where λ is latent heat (kJ kg^{-1}), Δ is the slope of the saturation vapour pressures curve (kPa °C^{-1}), γ is psychrometric constant (kPa °C^{-1}), *Rs* is the total solar radiation (MJ m^{-2} day^{-1}). These variables can be computed by equations in Allen et al. (1998):

$$R_S = K_t R_a \sqrt{T_{max} - T_{min}} \quad (6)$$

where T_{max} and T_{min} are the maximum and minimum air temperature (°C). *Kt* is the adjustment coefficient, *Kt* = 0.16, *Ra* is the extraterrestrial radiation (MJ m^{-2} day^{-1}) (Allen et al., 1998).

Being similar to the deduction of Hargreaves equation (Hargreaves and Samani, 1985), the simplified Makkink equation can be obtained by putting Eq. (8) into Eq. (4):

$$E_0 = 0.61K_t \cdot R_a \cdot \frac{\Delta}{\Delta+\gamma}\frac{\sqrt{T_{max} - T_{min}}}{\lambda} - 0.12 \quad (7)$$

Then the potential evaporation by the maximum and minimum temperature can be obtained by:

$$dE_0 \approx \frac{\partial g}{\partial T_{max}} dT_{max} + \frac{\partial g}{\partial T_{min}} dT_{min} \quad (8)$$

3.3. Quantification of impacts of precipitation and temperature on streamflow changes

The above-mentioned equations and also Eq. (4), the streamflow changes can be quantified by precipitation, maximum temperature (T_{max}) and minimum temperature (T_{min}) as:

$$\frac{dR}{R} = \varepsilon_P \frac{dP}{P} + \varepsilon_{T_{max}} \frac{dT_{max}}{T_{max}} + \varepsilon_{T_{min}} \frac{dT_{min}}{T_{min}} \quad (9)$$

where $\varepsilon_{T_{max}} = \varepsilon_{E_0} \frac{T_{max}}{E_0} \frac{\partial E_0}{\partial T_{max}}$, $\varepsilon_{T_{min}} = \varepsilon_{E_0} \frac{T_{min}}{E_0} \frac{\partial E_0}{\partial T_{min}}$. $\varepsilon_{T_{max}}$, $\varepsilon_{T_{min}}$ are the elasticity coefficients of the maximum, minimum temperature to streamflow changes.

Fractional contribution of precipitation and temperature to streamflow changes can be quantified by:

$$\Delta R_P = \varepsilon_P \overline{R}\frac{d\overline{P}}{\overline{P}}, \Delta R_T = \varepsilon_{T_{max}} \overline{R} d\overline{T_{max}} + \varepsilon_{T_{min}} \overline{R} d\overline{T_{min}} \quad (10)$$

where ΔR_P and ΔR_T are respectively precipitation- and temperature-induced streamflow changes with unit of mm. $d\overline{P}$ and $d\overline{T_{max}}$, $d\overline{T_{min}}$ denoted relative changes of long-term annual average precipitation (mm), maximum and minimum temperature (°C) during 2070–2099 when compared to those during 1960–1979. Meanwhile, fractional contribution rate of precipitation and temperature to streamflow changes can be computed by:

$$\delta R_P = \frac{\Delta R_P}{|\Delta R_P| + |\Delta R_T|} \times 100\%, \delta R_T = \frac{\Delta R_T}{|\Delta R_P| + |\Delta R_T|} \times 100\% \quad (11)$$

Three methods were applied to evaluate the effects of climate elasticities, they are Nash-Sutcliffe Efficiency (NSE), mean absolute error (MAE) and bias (Zhou et al., 2012). The indices can be obtained by:

$$NSE = 1 - \frac{\sum_{i=1}^{N}(Q_{obs,i} - Q_{sim,i})^2}{\sum_{i=1}^{N}(Q_{obs,i} - \overline{Q_{obs}})^2} \quad (12)$$

$$MAE = \frac{\sum_{i=1}^{N}|Q_{sim,i} - Q_{obs,i}|}{m} \quad (13)$$

$$bias = \frac{\sum_{i=1}^{N}(Q_{sim,i} - Q_{obs,i})}{\sum_{i=1}^{N} Q_{obs,i}} \times 100\% \quad (14)$$

where $Q_{obs,i}$ is the observed long-term mean streamflow change for the *i*th catchment, $Q_{sim,i}$ is the simulated long-term mean for the *i*th catchment, $\overline{Q_{obs}}$ is the average of observed streamflow change for all catchments, *N* is all the 37 tributaries across the Yellow River basin.

4. Results

4.1. Climatic elasticity to streamflow changes

Fig. 2 illustrates sensitivity of hydrological changes in Budyko framework. It can be seen from Fig. 2a that relations between the long-term annual average evaporation and the aridity index within 37 tributaries of the Yellow River follow the Budyko hydrothermal balance equation, i.e. Eq. (2). Under the condition of the fixed feature parameter, *n*, of a river basin, evaporation usually increases with increase of aridity index. In this sense, Budyko framework can be used in evaluation of impacts of climate change and human activities on streamflow changes, and also investigation of streamflow variations under future climatic scenarios. Fig. 2b shows spatial distribution of climatic elasticity of streamflow to precipitation and temperature, which can be calculated by Eqs. (3) and (9). Climatic elasticity reflects how sensitive of streamflow changes to external influencing factors. Spatial heterogeneity of elasticity index can be found in Fig. 2b. In general, climatic elasticity of streamflow changes in the middle and lower Yellow River basin is generally larger than that in the upper Yellow River basin. Specifically, climatic elasticity of streamflow changes in the Loess Plateau is larger than that in other regions of the Yellow River basin, implying the highest sensitivity of streamflow changes to climatic changes in the Loess Plateau. In the middle and lower Yellow River basin, the climatic elasticity of streamflow to precipitation ranges from 2 to 5, indicating that increase of 1% in precipitation can result in increase of 2–5% in streamflow. Meanwhile, climatic elasticity of streamflow to temperature in the middle and lower Yellow River basin lies between −5 and −1, showing that increase of 1 °C in temperature can result in decrease of 1–5% in streamflow. These results are in good line with those by Huang et al. (2016) and Yang et al. (2014). Similarly, Silberstein et al. (2012) indicated that increase of 1% in precipitation can cause increase of 2.9–3.5% in streamflow in river basins in southern Australia. Ma et al. (2010) also found that increase of 1 °C in temperature can lead to decrease of 4% in streamflow. Therefore, impacts of precipitation and temperature on streamflow changes are spatially similar to a large degree over the globe without consideration of human interferences.

4.2. Scenarios-based temperature and precipitation changes

Based on observed precipitation and temperature changes during 1960–2000, downscaling practice was done on outputs of 12 GCMs under RCP2.6 and RCP8.5 scenarios for a period of 2070–2099. Then Inverse Distance Weight spatial interpolation method was used to analyze spatial patterns of precipitation and temperature changes across the Yellow River basin (Fig. 3). It can be depicted from Fig. 3a that, under RCP2.6 scenario, increasing precipitation is dominant across the Yellow River basin. However, evident decrease of precipitation can be identified in the Hetao Plain with decreasing rate of 0%–20%. It should be noted here that Hetao Plain is the major agricultural zone, acting as the major supplier of agricultural products. Hence, predicted decreasing precipitation in

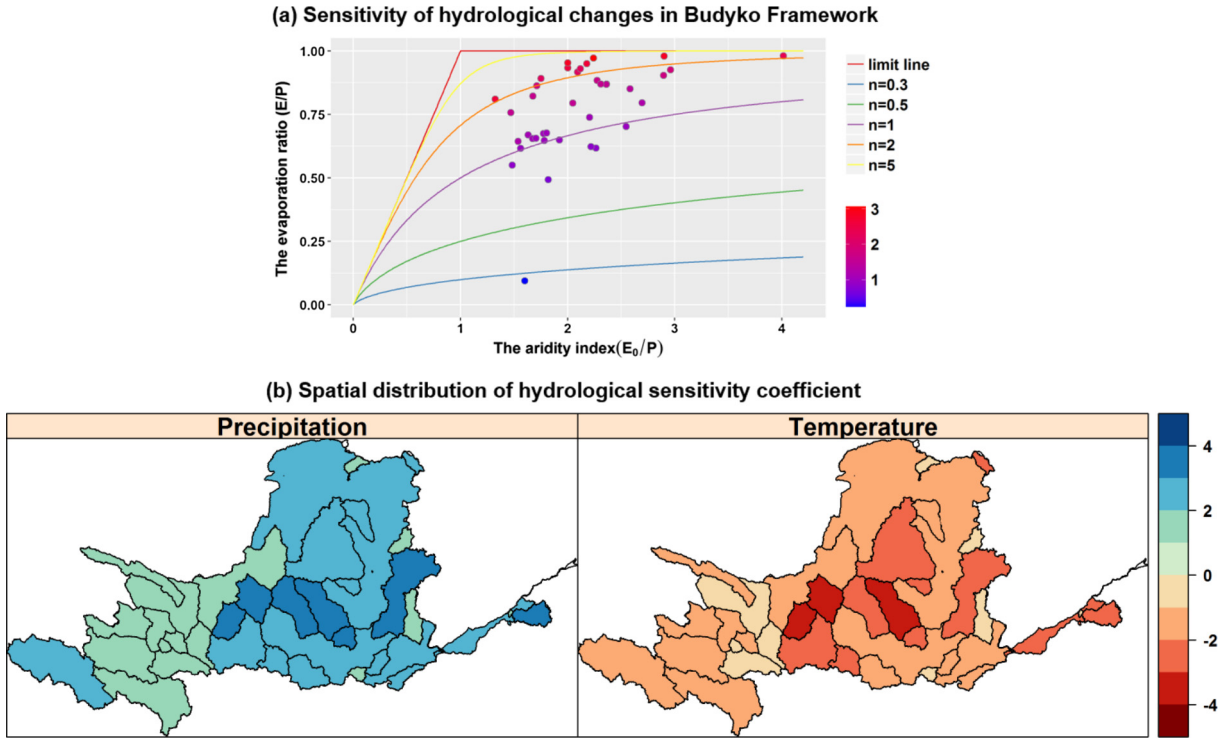

Fig. 2. Influence of climate variation on hydrological changes. (a) Relationship between evaporation ratio (E/P) and arid index (E_0/P)/catchment parameter *n*. The Budyko curves calculated by Eq. (2) are plotted as solid lines with different specific catchment parameter. Each point represents one catchment in the 37 catchments, the colour of the points corresponding to the colour bar refers to the value of *n* for each catchment. (b) Maps showing the climatic elasticity of streamflow to the changing precipitation and temperature in the 37 catchments. The streamflow elasticity to temperature is shown by the mean of ε_{Tmax} and ε_{Tmin}.

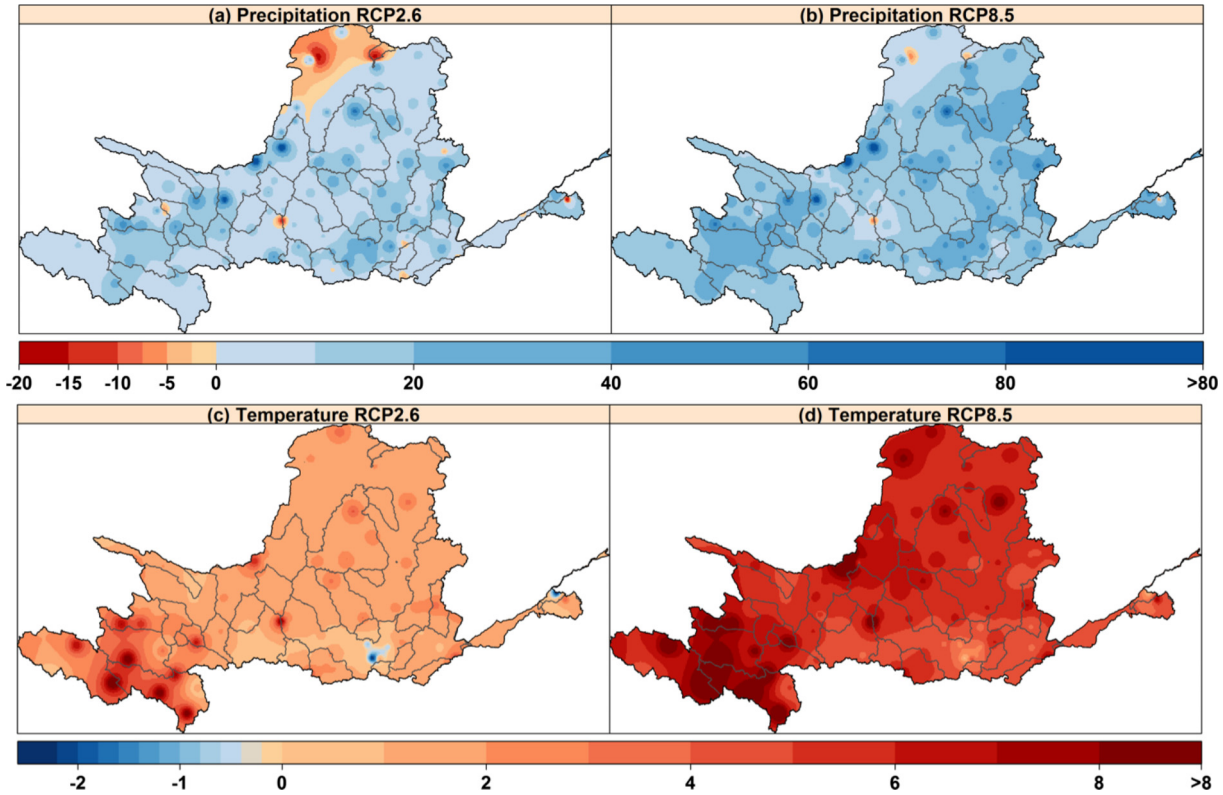

Fig. 3. Model ensemble median changes in precipitation (%) under (a) RCP2.6 and (b) RCP8.5, temperature (°C) under (c) RCP2.6 and (d) RCP8.5 during 2070–2099 relative to 1960–1979.

the Hetao Plain may have negative impacts on agricultural production. Under RCP8.5 scenario, however, larger areas of the Yellow River basin are characterized by increasing precipitation except some sporadic regions in the Yellow River basin (Fig. 3b). Besides, larger increasing magnitude of precipitation can be found under RCP8.5 when compared to that under RCP2.5 and most regions of the Yellow River basin under RCP8.5 are dominated by increasing magnitude of precipitation of 10–20%.

It can be seen from Fig. 3c and d that increasing temperature is obvious under different climatic scenarios. Under RCP2.6, increasing magnitude of temperature ranges between 1 and 3 °C and the increasing magnitude of global temperature is ~2 °C. Meanwhile, similar spatial patterns of temperature changes under RCP8.5 when compared to those under RCP2.6 but with larger increasing magnitude of temperature under RCP8.5 than that under RCP2.6. Increase of 4–6 °C in temperature can be identified under RCP8.5 and it is particularly the case for temperature changes in the headwater region of the Yellow River basin with increase of temperature of above 6 °C. These results are in good agreement with those by Sun et al. (2015) that increasing magnitude of temperature in most regions of the Yellow River basin under RCP8.5 will be above 4 °C.

4.3. Predicted streamflow under climatic scenarios

Downscaled precipitation and temperature were analyzed based on outputs of 12 GCMs under RCP2.6 and RCP8.5 scenarios, and predicted streamflow changes during 2070–2099 when compared to 1960–1979 period were obtained. Fig. 4 illustrates spatial pattern of median of predicted streamflow during 2070–2099 under RCP2.6 and RCP8.5 scenarios, which is obtained by Eq. (9). Under RCP2.6, increasing streamflow is dominant and streamflow in 26 out of 37 tributaries is increased with increase of <30 mm in streamflow depth and increasing magnitude of 0–20% (Fig. 4a, c). Increasing streamflow is found mainly in semi-humid and headwater regions of the Yellow River basin. Not significant increase of temperature but larger increasing magnitude of temperature combined to cause decreased streamflow in the Yellow River basin. Xu et al. (2009) evaluated streamflow changes during 2010–2099 using SWAT model, indicating that 2010–2099 period witnessed not evident increase of precipitation but significant increase of temperature and which is the major cause behind decreased streamflow in the headwater region of the Yellow River basin. Therefore, different researches are supposed to point to similar results concerning streamflow changes in the headwater region and related causes.

Under RCP8.5 scenario, more tributaries are dominated by increased streamflow with larger increasing magnitude of the streamflow depth between 10 and 40 mm. The increasing rate of streamflow ranges between 20 and 30% (Fig. 4b, d). Streamflow changes shift from decrease under RCP2.6 to increase under RCP8.5, and which can be attributed to more significant increase of precipitation under RCP8.5 than that under RCP2.6. Besides, there are 8 tributaries dominated by decreased streamflow under RCP8.5 and these tributaries mainly concentrate in the middle Yellow River basin. It should be noted here that 40% of the cropland within the Yellow River basin is heavily dependent on irrigation and hence decreased streamflow may have negative implications for development of irrigated agriculture. Above-mentioned results imply that higher emission of greenhouse gas can cause larger climatic impacts, precipitation in this study, on streamflow changes and this viewpoint was well corroborated by results by Teng et al. (2012) in Australia.

Fig. 5 shows spatial distribution of fractional contribution rate of precipitation and temperature (calculated by Eq. (10)) to changes of predicted streamflow across the Yellow River basin. In general, precipitation tends to increase streamflow and temperature tends to decrease streamflow of the Yellow River basin. Meanwhile, fractional contribution of precipitation to streamflow changes is generally larger than that of temperature to streamflow

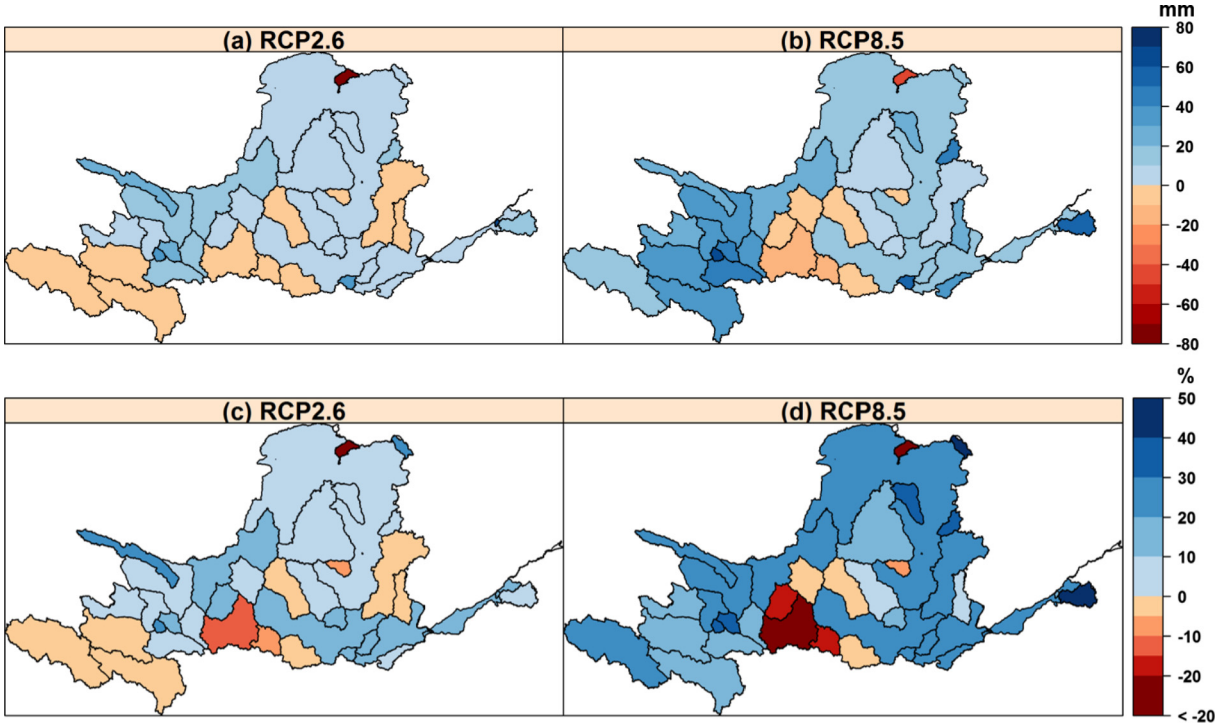

Fig. 4. Model ensemble median change (mm) of streamflow under (a) RCP2.6 and (b) RCP8.5 and percentage change in streamflow (%) under (c) RCP2.6 and (d) RCP8.5 during 2070–2099 relative to during 1960–1979. The colourful dots indicate the changing significance, the 'significant' change is determined by the changing magnitude larger than one standard deviation.

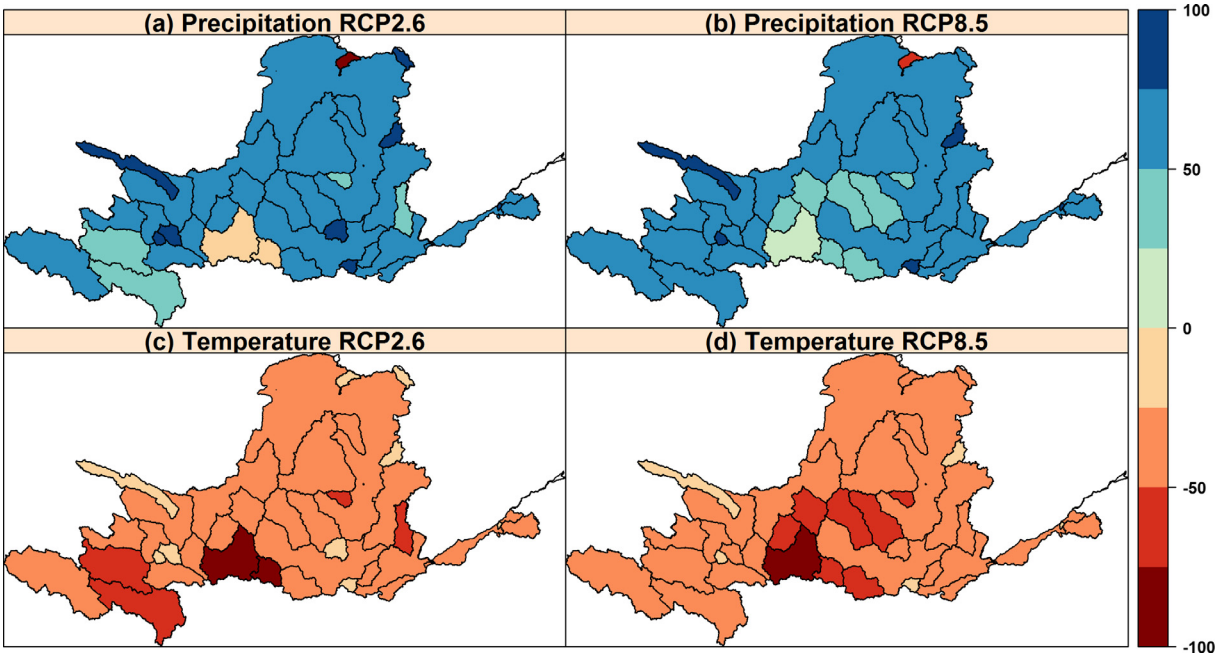

Fig. 5. Contribution of precipitation change to streamflow change by multi-model ensemble median under (a) RCP2.6 and (b) RCP8.5, as well as annual temperature change under (c) RCP2.6 and (d) RCP8.5 during 2070–2099 relative to 1960–1979.

changes. Under RCP8.5 and RCP2.6 scenarios, fractional contribution rates of precipitation to streamflow changes are respectively 64.8% and 68.4%. However, spatial patterns of fractional contribution rate of temperature and precipitation to streamflow changes are similar in general. Moreover, fractional contribution of temperature to streamflow changes under RCP8.5 is larger than that under RCP2.6. In addition, under RCP8.5, fractional contribution rate of temperature to streamflow changes in the middle Yellow River basin is larger than precipitation, causing decreasing streamflow in these tributaries of the middle Yellow River basin.

4.4. Uncertainty evaluation

Uncertainty due to outputs of GCMs is usually larger than that stemmed from hydrological modelling procedure (e.g. Li et al., 2016). Hawkins and Sutton (2009) showed that uncertainty related to GCMs includes climatic models, climatic scenarios and ensemble, and uncertainty related to climatic models is the most significant one. Therefore, this study attempted to address uncertainty evaluation via comparison of streamflow changes based on outputs of different GCMs. Fig. 6 demonstrated spatial distribution of changing rate of streamflow during 2070–2099 relative to during 1960–1979 based on outputs of 12 GCMs under RCP2.6 and RCP8.5 scenarios. It can be well discerned from Fig. 6 that scenario-based climatic changes have remarkable impacts on streamflow changes in the future, a period of 2070–2099 in this study. However, discernable differences can be expected for climatic impacts on streamflow changes based on different GCMs. Under RCP2.6, decreased streamflow is dominant within the Yellow River basin based on outputs of these five GCMs, i.e. BCC-CSM1.1 (m), CCSM4, CSIRO-Mk3.6.0, IPSL-CM5A-MR, MPI-ESM-M and MRI-CGCM3. However, increased streamflow is dominant within the Yellow River basin based on outputs of the rest 7 GCMs. Under RCP8.5 however, except CSIRO-Mk3.6.0, IPSL-CM5A-MR and MPI-ESM-M, outputs of other 9 GCMs can cause increased streamflow of the Yellow River basin. Specifically, based on outputs of BNU-ESM and MIROC5, streamflow of all tributaries of the Yellow River basin is increasing.

Fig. 7 presented change rates of precipitation, temperature and streamflow as well based 12 GCMs under RCP2.6 during 2070–2099 relative to 1960–1979 period. It can be seen from Fig. 7 that smaller difference can be observed for average temperature changes based on GCMs in the Yellow River basin, and the changing magnitude of temperature is 1.4–6.8%. However, remarkable difference of precipitation changes based on different GCMs can be identified. Specifically, increase of 20% of the long-term annual average precipitation can be observed based on outputs of CanESM2 and CNRM-CM5 models. However, based on outputs of CSIRO-Mk3.6.0 model, decrease of streamflow of 4% can be observed. In this sense, uncertainty in evaluation of climatic impacts on streamflow changes can be attributed mainly to precipitation changes modelled by GCMs. Though standing uncertainty in evaluation of climatic impacts on streamflow changes, changing properties of streamflow in different tributaries of the Yellow River basin are similar. Fig. 8 showed spatial distribution of the number of models that have the outputs causing increased streamflow in tributaries of the Yellow River basin. It can be depicted from Fig. 8 that similar streamflow changes can be obtained based on outputs of above 2/3 of the GCMs and in this case confirmed results can be expected (Arnell and Gosling, 2013). Under RCP2.6, increased streamflow can be detected in 36.8% of the tributaries considered in this study and decreased streamflow can be observed in 7.9% of the tributaries considered in this study. Comparatively, under RCP8.5, 71.1% of the tributaries of the Yellow River basin are dominated by increased streamflow.

5. Discussions

To further verify applicability of Budyko assumption in modelling streamflow changes as results of precipitation and temperature, observed streamflow changes were used to evaluate modelling performance of Budyko framework in simulation of streamflow changes of the Yellow River basin. Fig. 9 showed relations between modelled streamflow ($\Delta R_P + \Delta R_n + \Delta R_T$) and observed streamflow during 1980–2000 relative to 1960–1979. Pretty good match of modelled to observed streamflow can be

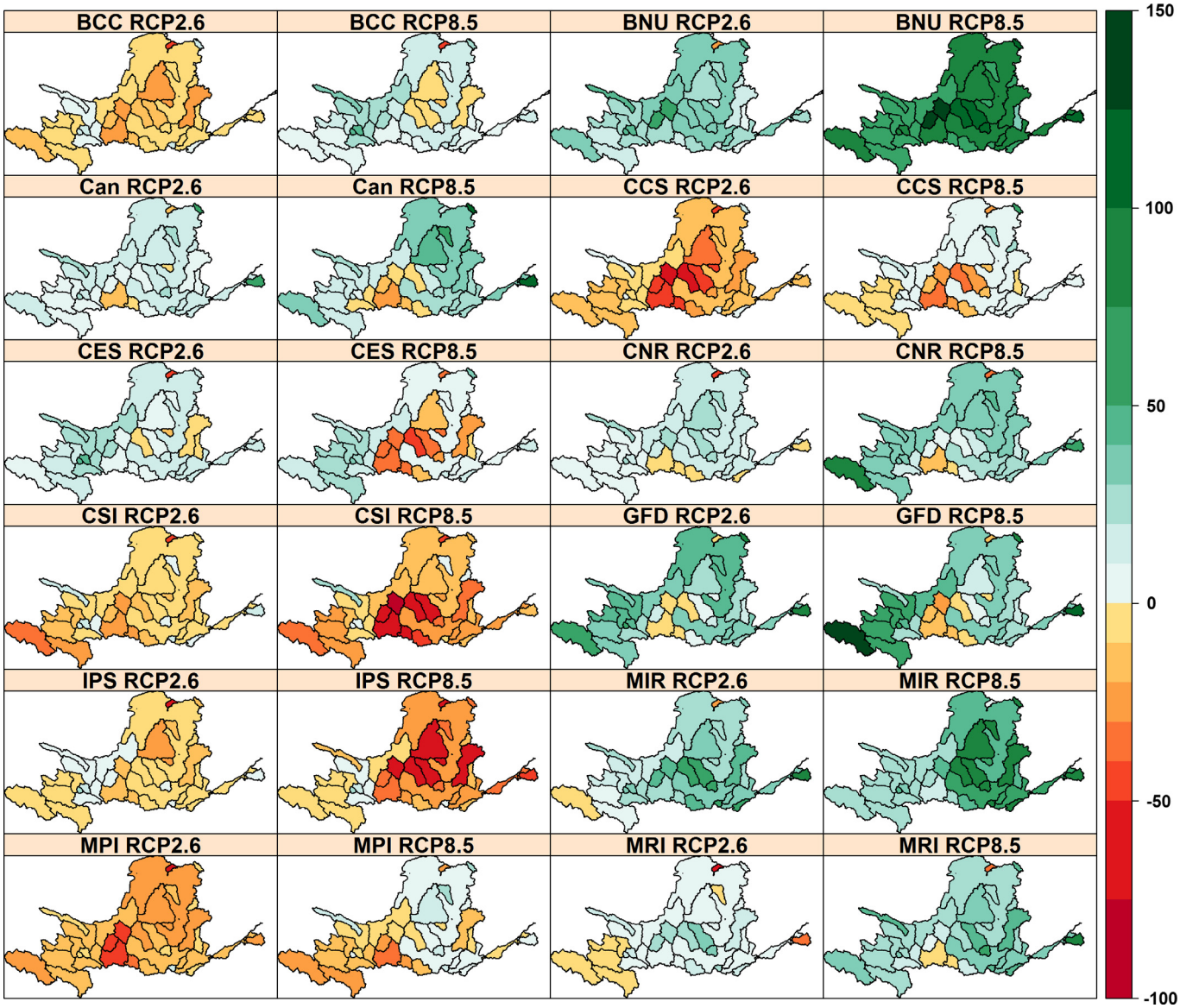

Fig. 6. Percentage change of projected future runoff across China by 12 GCMs under RCP26 and RCP8.5. BCC, BNU, Can, CCS, CES, CNR, CSI, GFD, IPS, MIR, MPI and MRI denote BCC-CSM1.1 (m), BNU-ESM, CanESM2, CCSM4, CESM1 (CAM5), CNRM-CM5, CSIRO-Mk3.6.0, GFDL-CM3, IPSL-CM5A-MR, MIROC5, MPI-ESM-M and MRI-CGCM3, respectively.

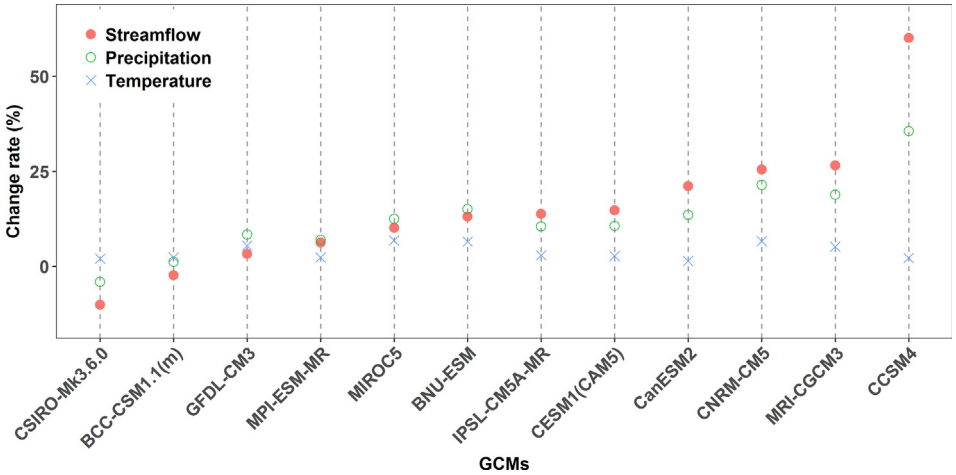

Fig. 7. Uncertainty in the proportion of station with increased runoff by 12 GCMs under RCP2.6 in the 10 rivers basin.

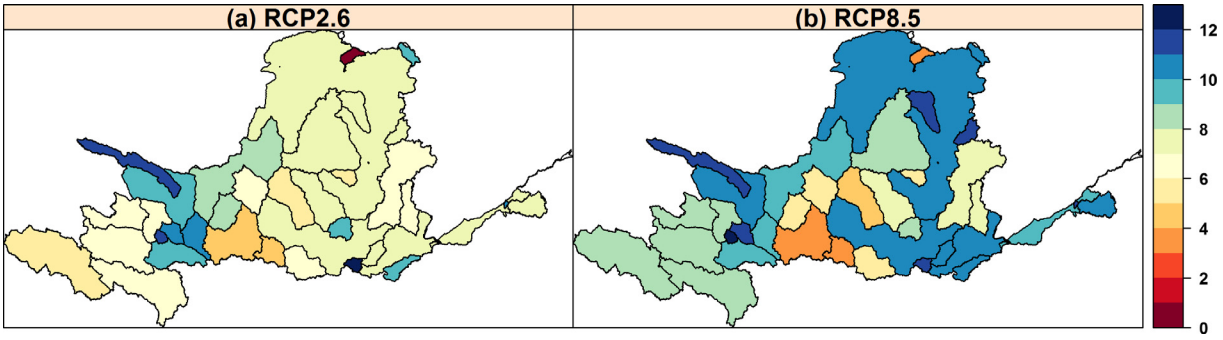

Fig. 8. Numbers of ensemble members out of 12 climate models showing an increase in future annual runoff under (a) RCP2.6 and (b) RCP8.5.

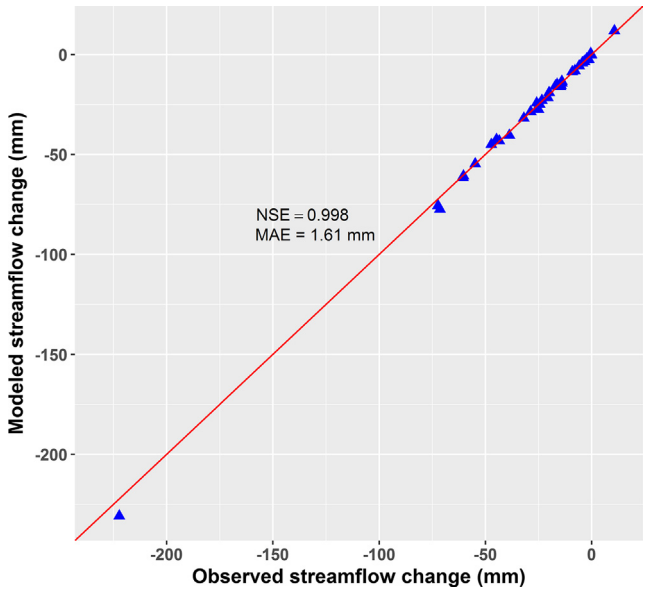

Fig. 9. The cross comparison of simulated runoff change ($\Delta R_P + \Delta R_n + \Delta R_T$) and observed ones in during 1980–2000 related to during 1960–1979, the red line is a 1:1 straight line. It is worth noting that the goodness-of-fit indices, i.e., NSE and MAE are used to assess the performance of long-term mean simulated streamflow change for 37 tributaries across Yellow river, which is calculated by Eqs. (12-14).

observed from Fig. 9 with correlation coefficient of 0.998 and mean error of 1.61 mm, implying that Budyko framework can be well used in modelling streamflow changes in the Yellow River basin. Wang et al. (2016), based on Budyko framework and FAO56 Penman equation, deduced climatic elasticity method with 7 parameters such as precipitation, underlying surface parameter and also other 5 evaporation factors including solar radiation, wind speed, relative humidity, maximum and minimum temperature, or simply Pn5 in this study. Li et al. (2017a,b) used the Budyko framework in differentiating influencing factors for observed streamflow changes of the Yellow River basin, showing that Budyko framework performs well in modelling observed streamflow changes and related influencing factors. To further clarify modelling performance of the Budyko-based model developed in this study, or simply PnT in this current study, comparison was done between results of this current study and those by Wang et al. (2016) (Fig. 10a). Besides, the original Budyko framework was denoted simply as PnE. It can be seen from Fig. 10 that the modelling error of streamflow by PnT in 25 out of 37 tributaries of the Yellow River basin is smaller than that by Pn5. In addition, PnT and Pn5 generally stemmed from PnE (Yang et al., 2008a,b; Xu et al., 2014), and hence comparison was also done on results by PnT and those by PnE (Fig. 10b). It can be seen from Fig. 10b that modelling error of streamflow by PnT is mostly larger than that by PnE in most tributaries of the Yellow River basin. Therefore, from a perspective of absolute error, PnT performs better than Pn5 does. Based on deviation coefficient, PnT has similar performance with PnE.

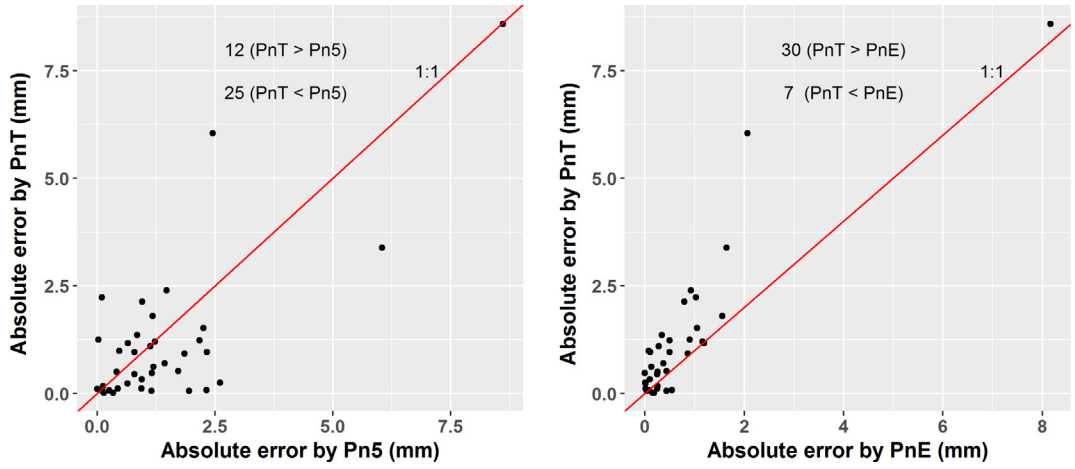

Fig. 10. Comparison of the PnT four-parameter elasticity method with (a) the Pn5 seven-parameter elasticity method and (b) the PnE_0 three-parameter elasticity method in simulating runoff change during 1980–2000 related to 1960–1979 in 37 catchments across China.

Table 2
Summary of model performance for the PnT four-parameter elasticity method, the Pn5 even-parameter elasticity method and the PnE three-parameter elasticity method. The assessment methods of NSE, MAE and bias are applied to evaluate the predicted effect of long-term mean simulated streamflow change for different catchments, which are calculated by Eqs. (12-14).

	PnT	Pn5	PnE
Nash-Sutcliffe efficiency efficient	0.997	0.997	0.998
Mean absolute error (mm)	1.162	1.401	0.703
Bias (%)	−1.53	−4.6	−1.4

However, the deviation coefficient of the modelled streamflow by Pn5 is relatively larger (Table 2). Moreover, Nash results for PnE, PnT and Pn5 are all larger than 0.9, showing acceptable modelling results.

However, it should be noted here that this current study aims to addressing prediction of streamflow changes of the Yellow River basin. Liu and Sun (2016) indicated that potential evaporation results by GCMs contains remarkable uncertainty. Outputs of GCMs usually underestimate solar radiation and overestimate wind speed, vapor pressure deficit and also temperature, and hence underestimated potential evaporation. However, potential evaporation is one of the critical parameters for PnE. Pn5 contains 7 parameters and 6 meteorological variables are needed in modelling, which implies extra error and uncertainty. In addition, more inputs of GCMs outputs also have the potential to introduce more uncertainty (Wang et al., 2015, 2016). Comparatively, PnT method developed in this study need less inputs of meteorological variables, i.e. precipitation, maximum and minimum temperature only. Moreover, temperature by GCMs contains the least uncertainty and plays a most important role in the increase of evaporation in the Yellow River basin (Wang et al., 2012a,b). In this sense, PnT developed in this study is the right choice for the research objectives of this current study. However, it should be clarified here that only climatic changes under climatic scenarios were taken into account in hydrological modelling. Changes of underlying surface properties and also human activities were not included. Zhang et al. (2009a) indicated that vegetation changes also impact fluvial hydrological cycle and hence have impacts on streamflow changes. Therefore, predicted streamflow changes in this current study are the results mainly by climatic changes. Human impacts and changes of underlying surface properties are hard to be evaluated and predicted. Inclusion of these factors has the potential to introduce more uncertainty (Davie et al., 2013; Kumar et al., 2016).

6. Conclusions

This study attempted to address prediction of streamflow changes during 2070–2099 relative to 1960–1979 in the Yellow River basin under RCP8.5 and RCP2.6 scenarios using Budyko framework and outputs of 12 GCMs were analyzed. Some important and interesting conclusions can be obtained as follows:

(1) During 2070–2099, long-term annual average precipitation is in evident variations. Under RCP2.6, increased precipitation can be detected in most regions of the Yellow River basin. Furthermore, larger increasing magnitude of precipitation can be found in more regions under RCP8.5 than those under RCP2.6. Specifically, increase of 10% in precipitation amount can be detected in most regions of the Yellow River basin under RCP8.5. Therefore, increased precipitation can be expected during 2070–2099 and it is particularly true under influences of larger human emission of greenhouse gas such as RCP8.5 in this study. Similarly, increased temperature can be identified under RCP2.6 and RCP8.5 scenarios. Particularly, increase of >3 °C of temperature can be detected under RCP8.5.

(2) Climatic elasticity method developed in this study using Budyko framework performs well in modelling and prediction of streamflow changes in the Yellow River basin. The modelled streamflow match well the observed streamflow changes. The climatic elasticity of the streamflow to climatic changes in the Loess Plateau is higher than other regions of the Yellow River basin, showing higher sensitivity of streamflow changes to climate changes in the Loess Plateau. In general, increase of 1% in precipitation amount can cause increase of 2–5% in streamflow; meanwhile, increase of 1 °C in temperature can result in decrease of 1–5% of the streamflow.

(3) Increasing streamflow during 2070–2099 can be expected and number of tributaries with increasing streamflow and also increasing magnitude of streamflow are larger under RCP8.5 than those under RCP2.6. In semi-humid regions and the headwater region as well of the Yellow River basin, significant increase of temperature but slight increase of precipitation cause decreased streamflow. Fractional contribution rate of temperature to streamflow changes in these two regions is >50%.

(4) Results of this study showed distinct different pictures for streamflow changes considering outputs of different GCMs. The uncertainty in predicted streamflow changes can be attributed mainly to different precipitation outputs from different GCMs. Even so, majority outputs of GCMs indicated increasing streamflow under RCP2.6 and RCP8.5 with different increasing magnitude. Under RCP2.6, 36.8% of the tributaries of the Yellow River are characterized by persistently increasing streamflow; Under RCP8.5 however, 71.1% of the tributaries of the Yellow River basin are dominated by increasing streamflow with larger increasing magnitude. The results of this stud are of theoretical and practical merits in terms of management of water resources and also irrigated agriculture under influences of changing climate.

Acknowledgments

This work is financially supported by the National Science Foundation for Distinguished Young Scholars of China (Grant No.: 51425903), the Fund for Creative Research Groups of National Natural Science Foundation of China (Grant No.: 41621061) and by National Science Foundation of China (Grant No.: 41771536). Our cordial gratitude should be extended to the editor, Prof. Dr. Geoff Syme, and anonymous reviewers for their professional and pertinent comments and revision suggestions which are greatly helpful for further quality improvement of this manuscript.

References

Ahn, K., Merwade, V., 2014. Quantifying the relative impact of climate and human activities on streamflow. J. Hydrol. 515, 257–266.
Allen, R.G., Pereira, L.S., Raes, D., Smith, M., 1998. Crop evapotranspiration-Guidelines for computing crop water requirements-FAO Irrigation and drainage paper 56. FAO, Rome 300 (9), D05109.
Arnell, N.W., Gosling, S.N., 2013. The impacts of climate change on river flow regimes at the global scale. J. Hydrol. 486, 351–364.
Bates, B., Kundzewicz, Z.W., Wu, S., Palutikof, J., 2008. Climate change and water. Intergovernmental Panel on Climate Change (IPCC).
Boczon, A., Brandyk, A., Wrobel, M., Kowalska, A., 2015. Transpiration of a stand and evapotranspiration of Scots pine ecosystem in relation to the potential evapotranspiration estimated with different methods. SYLWAN 159 (8), 666–674.
Budyko, M., 1974. Climate and Life. Academic Press, New York. 508 pp.

Chen, J., Xia, J., Zhao, C., Zhang, S., Fu, G., Ning, L., 2014. The mechanism and scenarios of how mean annual runoff varies with climate change in Asian monsoon areas. J. Hydrol. 517, 595–606.
Chiew, F.H., 2006. Estimation of rainfall elasticity of streamflow in Australia. Hydrol. Sci. J. 51 (4), 613–625.
Davie, J.C.S., Falloon, P.D., Kahana, R., Dankers, R., Betts, R., Portmann, F.T., Wisser, D., Clark, D.B., Ito, A., Masaki, Y., Nishina, K., Fekete, B., Tessler, Z., Wada, Y., Liu, X., Tang, Q., Hagemann, S., Stacke, T., Pavlick, R., Schaphoff, S., Gosling, S.N., Franssen, W., Arnell, N., 2013. Comparing projections of future changes in runoff from hydrological and biome models in ISI-MIP. Earth System Dynamics 4, 359–374.
De Bruin, H., Lablans, W., 1998. Reference crop evapotranspiration determined with a modified Makkink equation. Hydrol. Process. 12 (7), 1053–1062.
Frans, C., Istanbulluoglu, E., Mishra, V., Munoz-Arriola, R., Lettenmaier, D.P., 2013. Are climatic or land cover changes the dominant cause of runoff trends in the Upper Mississippi River Basin? Geophys. Res. Lett. 40, 1104–1110.
Gao, Z., Zhang, L., Zhang, X., Cheng, L., Potter, N., Cowan, T., Cai, W., 2016. Long-term streamflow trends in the middle reaches of the Yellow River Basin: detecting drivers of change. Hydrol. Process. 30 (9), 1315–1329.
Hargreaves, G.H., Samani, Z.A., 1985. Reference crop evapotranspiration from temperature. Appl. Eng. Agric. 1 (2), 96–99.
Hawkins, E., Sutton, R., 2009. The potential to narrow uncertainty in regional climate predictions. Bull. Am. Meteorol. Soc. 90 (8), 1095–1107.
Huang, Z., Yang, H., Yang, D., 2016. Dominant climatic factors driving annual runoff changes at the catchment scale across China. Hydrol. Earth Syst. Sci. 20 (7), 2573–2587.
IPCC, 2007. Climate Change 2007: The Physical Science Basis. Cambridge University Press. 996 pp.
Kumar, S., Zwiers, F., Dirmeyer, P.A., Lawrence, D.M., Shrestha, R., Werner, A.T., 2016. Terrestrial contribution to the heterogeneity in hydrological changes under global warming. Water Resour. Res. 52 (4), 3127–3142.
Li, B., Li, C., Liu, J., Zhang, Q., Duan, L., 2017a. Decreased streamflow in the yellow river basin, china: climate change or human-induced? Water 116. https://doi.org/10.3390/w9020116.
Li, F., Zhang, Y., Xu, Z., Teng, J., Liu, C., Liu, W., Mpelasoka, F., 2013. The impact of climate change on runoff in the southeastern Tibetan Plateau. J. Hydrol. 505, 188–201.
Li, H., Zhang, Q., Singh, V.P., Shi, P., Sun, P., 2017b. Hydrological effects of cropland and climatic changes in arid and semi-arid river basins: a case study from the Yellow River basin, China. J. Hydrol. 549, 547–557.
Li, J., Chen, Y.D., Zhang, L., Zhang, Q., Chiew, F.H., 2016. Future changes in floods and water availability across China: linkage with changing climate and uncertainties. J. Hydrometeorol. 17 (4), 1295–1314.
Liang, K., Liu, C., Liu, X., Song, X., 2013. Impacts of climate variability and human activity on streamflow decrease in a sediment concentrated region in the Middle Yellow River. Stoch. Environ. Res. Risk Assess. 27 (7), 1741–1749.
Liu, Q., Cui, B., 2011. Impacts of climate change/variability on the streamflow in the Yellow River Basin China. Ecol. Modell. 222 (2), 268–274.
Liu, J., Zhang, Q., Singh, V.P., Shi, P., 2017. Contribution of multiple climatic variables and human activities to streamflow changes across China. J. Hydrol. 545, 145–162.
Liu, W., Sun, F., 2016. Assessing estimates of evaporative demand in climate models using observed pan evaporation over China. J. Geophys. Res. 121 (14), 8329–8349.
Ma, H., Yang, D., Tan, S.K., Gao, B., Hu, Q., 2010. Impact of climate variability and human activity on streamflow decrease in the Miyun Reservoir catchment. J. Hydrol. 389 (3), 317–324.
Makkink, G.F., 1957. Testing the Penman formula by means of lysimeters. J. Water Process Eng. 11 (3), 277–288.
Mehrotra, R., Sharma, A., Kumar, D.N., Reshmidevi, T., 2013. Assessing future rainfall projections using multiple GCMs and a multi-site stochastic downscaling model. J. Hydrol. 488, 84–100.
Naz, B.S., Kao, S.C., Ashfaq, M., Rastogi, D., Mei, R., Bowling, L.C., 2016. Regional hydrologic response to climate change in the conterminous United States using high-resolution hydroclimate simulations. Global Planet. Change 143, 100–117.
Novotny, E.V., Stefan, H.G., 2007. Stream flow in Minnesota: indicator of climate change. J. Hydrol. 334, 319–333.
Reichler, T., Kim, J., 2008. How well do coupled models simulate today's climate? Bull. Am. Meteorol. Soc. 89 (3), 303–311.
Riahi, K., Rao, S., Krey, V., Cho, C., Chirkov, V., Fischer, G., Kindermann, G., Nakicenovic, N., Rafaj, P., 2011. RCP 8.5-A scenario of comparatively high greenhouse gas emissions. Climatic Change 109, 33–57.
Ryberg, K.R., Lin, W., Vecchia, A.V., 2013. Impact of climate variability on runoff in the North Central United States. J. Hydrol. Eng. 19 (1), 148–158.
Sankarasubramanian, A., Vogel, R.M., Limbrunner, J.F., 2001. Climate elasticity of streamflow in the United States. Water Resour. Res. 37 (6), 1771–1781.
Silberstein, R., Aryal, S.K., Durrant, J., Pearcey, M., Braccia, M., Charles, S.P., Boniecka, L., Hodgson, G.A., Bari, M.A., Viney, N.R., McFarlaneet, D.J., 2012. Climate change and runoff in south-western Australia. J. Hydrol. 475, 441–455.
Sun, Q., Miao, C., Duan, Q., 2015. Projected changes in temperature and precipitation in ten river basins over China in 21st century. Int. J. Climatol. 35 (6), 1125–1141.
Taylor, K.E., Stouffer, R.J., Meehl, G.A., 2012. An overview of CMIP5 and the experiment design. Bull. Am. Meteorol. Soc. 93 (4), 485–498.
Tang, Y., Tang, Q., Tian, F., Zhang, Z., Liu, G., 2013. Responses of natural runoff to recent climatic variations in the Yellow River basin, China. Hydrol. Earth Syst. Sci. 17, 4471–4480.
Teng, J., Chiew, F.H.S., Vaze, J., Marvanek, S., Kirono, D.G.C., 2012. Estimation of climate change impact on mean annual runoff across continental Australia using Budyko and Fu equations and hydrological models. J. Hydrometeorol. 13 (3), 1094–1106.
van Vuuren, D.P., Edmonds, J., Kainuma, M., Riahi, K., Thomson, A., Hibbard, K., Hurtt, G.C., Kram, T., Krey, V., Lamarque, J.-F., Masui, T., Meinshausen, M., Nakicenovic, N., Smith, S.J., Rose, S.K., 2011. The representative concentration pathways: an overview. Climatic Change 109, 5–31.
Wang, G.Q., Wang, Y.Z., Shi, Z.H., Kang, L.L., Li, H.B., 2001. Analysis on water resources variation tendency in the Yellow River. Sci. Geog. Sin. 21 (5), 396–400 (in Chinese with English abstract).
Wang, S., Yan, M., Yan, Y., Shi, C., He, L., 2012a. Contributions of climate change and human activities to the changes in runoff increment in different sections of the Yellow River. Quat. Int. 282, 66–77.
Wang, W., Shao, Q., Peng, S., Xing, W., Yang, T., Luo, Y., Yong, B., Xu, J., 2012b. Reference evapotranspiration change and the causes across the Yellow River Basin during 1957–2008 and their spatial and seasonal differences. Water Resour. Res. 48 (5), W05530. https://doi.org/10.1029/2011WR010724.
Wang, W., Xing, W., Shao, Q., 2015. How large are uncertainties in future projection of reference evapotranspiration through different approaches? J. Hydrol. 524, 696–700.
Wang, W., Zou, S., Shao, Q., Xing, W., Chen, X., Jiao, X., Luo, Y., Yong, B., Yu, Z., 2016. The analytical derivation of multiple elasticities of runoff to climate change and catchment characteristics alteration. J. Hydrol. 541, 1042–1056.
Winter, T., Rosenberry, D., Sturrock, A., 1995. Evaluation of 11 equations for determining evaporation for a small lake in the north central United States. Water Resour. Res. 31 (4), 983–993.
Xu, J.X., 2001. High-frequency zone of river desiccation disasters in China and the influencing factors. Environ. Manage. 28, 101–113.
Xu, J.X., 2002. River sedimentation and channel adjustment of the lower Yellow River as influenced by low discharges and seasonal channel dry-ups. Geomorphology 43, 151–164.
Xu, C.-Y., Singh, V.P., 2000. Evaluation and generalization of radiation-based methods for calculating evaporation. Hydrol. Processes 14 (2), 339–349.
Xu, C.-Y., Singh, V.P., 2002. Cross comparison of empirical equations for calculating potential evapotranspiration with data from Switzerland. Water Resour. Manage 16 (3), 197–219.
Xu, C.-Y., Chen, D., 2005. Comparison of seven models for estimation of evapotranspiration and groundwater recharge using lysimeter measurement data in Germany. Hydrol. Processes 19 (18), 3717–3734.
Xu, Z., Zhao, F., Li, J., 2009. Response of streamflow to climate change in the headwater catchment of the Yellow River basin. Quat. Int. 208 (1), 62–75.
Xu, X., Yang, D., Yang, H., Lei, H., 2014. Attribution analysis based on the Budyko hypothesis for detecting the dominant cause of runoff decline in Haihe basin. J. Hydrol. 510, 530–540.
Yang, H., Yang, D., 2011. Derivation of climate elasticity of runoff to assess the effects of climate change on annual runoff. Water Resour. Res. 47 (7), W07526. https://doi.org/10.1029/2010wr009287.
Yang, H., Qi, J., Xu, X., Yang, D., Lv, H., 2014. The regional variation in climate elasticity and climate contribution to runoff across China. J. Hydrol. 517, 607–616.
Yang, H., Yang, D., Lei, Z., Sun, F., 2008a. New analytical derivation of the mean annual water-energy balance equation. Water Resour. Res. 44 (3), W03410. https://doi.org/10.1029/2007wr006135.
Yang, T., Zhang, Q., Chen, Y.D., Tao, X., Xu, C.-Y., Chen, X., 2008b. A spatial assessment of hydrologic alteration caused by dam construction in the middle and lower Yellow River, China. Hydrol. Processes 22 (18), 3829–3843.
Zhang, L., Zhao, F., Chen, Y., Dixon, R.N., 2009a. Estimating effects of plantation expansion and climate variability on streamflow for catchments in Australia. Water Resour. Res. 47, W12539. https://doi.org/10.1029/2011WR010711.
Zhang, Q., Xu, C.-Y., Yang, T., 2009b. Variability of water resource in the Yellow River basin of past 50 years, China. Water Resour. Manage. 23 (6), 1157–1170.
Zhang, Q., Gu, X., Singh, V.P., Xu, C.-Y., Kong, D., Xiao, M., Chen, X., 2015a. Homogenization of precipitation and flow regimes across China: changing properties, causes and implications. J. Hydrol. 530, 462–475.
Zhang, Y., Fu, G., Sun, B., Zhang, S., Men, B., 2015b. Simulation and classification of the impacts of projected climate change on flow regimes in the arid Hexi Corridor of Northwest China. J. Geophys. Res.: Atmos. 120 (15), 7429–7453.
Zhang, Q., Liu, J., Singh, V.P., Gu, X., Chen, X., 2016. Evaluation of impacts of climate change and human activities on streamflow in the Poyang Lake basin, China. Hydrol. Processes. 10.1002/hyp.10814.
Zhang, X., Tang, Q., Zhang, X., Lettenmaier, D.P., 2014. Runoff sensitivity to global mean temperature change in the CMIP5 Models. Geophys. Res. Lett. 41 (15), 5492–5498.
Zheng, H., Zhang, L., Zhu, R., Liu, C., Sato, Y., Fukushima, Y., 2009. Responses of streamflow to climate and land surface change in the headwaters of the Yellow River Basin. Water Resour. Res. 45 (7), W00A19. https://doi.org/10.1029/2007WR006665.
Zhou, X., Zhang, Y., Wang, Y., Zhang, H., Vaze, J., Zhang, L., Yang, Y., Zhou, Y., 2012. Benchmarking global land surface models against the observed mean annual runoff from 150 large basins. J. Hydrol. 470, 269–279.
Zhou, Y., Zhang, Q., Singh, V.P., 2014. Fractal-based evaluation of the effect of water reservoirs on hydrological processes: the dams in the Yangtze River as a case study. Stochastic Environ. Res. Risk Assess. 28, 263–279.